

NODAL LINE FINITE DIFFERENCE METHOD FOR THE ANALYSIS
OF PLATES WITH VARIABLE FLEXURAL RIGIDITY

BY

DR. ENG. YOUSSEF AGAG *

INTRODUCTION

The application of semi-analytical methods for the analysis of two and three dimensional structural problems has been the subject of considerable research interest in recent years. These methods are especially advantageous for the structures having regular geometric planes and simple boundary conditions. The finite strip method as a semi-analytical procedure has been recently developed by CHEUNG [1,2]. This method can be considered as a special form of the finite element procedure using the displacement approach. Unlike the finite element method, which uses polynomial displacement functions in all directions, the finite strip method calls for use of simple polynomials across the width of the strip and harmonic series in the longitudinal direction. These series should satisfy a priori the boundary conditions at the ends of the strip. The most common series used are the basic functions, which are derived from the solution of beam vibration differential equation. These basic functions have been worked out explicitly by VLAZOV [3] for the various end conditions. This method has proved to be an economical and accurate means of treating a class of structural problems.

More recently a new semi-analytical procedure named "The nodal line finite difference method" (N.L.F.D) has been developed by the author [4] for the analysis of elastic plates with two opposite simply supported ends. In this analysis, a trigonometric series is used to express the displacement variation along the nodal lines. Basic function other than trigonometric series, is used by the author [5] to analyze elastic plates with two opposite clamped ends. In this analysis, an iteration procedure has been used to overcome the coupling property of the static equilibrium equations. The nodal line finite difference method permits the direct formulation of the plate bending problems by reducing the partial differential equation to an ordinary differential equation. This method is similar to that the finite strip method since each uses harmonic series to express the displacement variation along the nodal lines. The nodal line finite difference method has an advantage over the finite strip method, since the number of the unknown parameters along a nodal line in this method is equal to the number of terms used in the basic function. This is greatly less than that of the finite strip method.

* Lecturer, Struct. Eng. Dept. Mansoura University, Egypt

The object of the present work is to demonstrate the versatility of the nodal line finite difference method in the analysis of plates with variable flexural rigidity. In general, variable flexural rigidity creates numerous mathematical difficulties. The complexity of the "exact" solution depends considerably on the expressions representing the flexural rigidity and that of the applied loading. The problems related to plates with variable flexural rigidity can seldom be solved by the analytical methods. Consequently the solutions are usually obtained via approximate and numerical techniques.

The proposed technique is used to analyze rectangular plates with variable flexural rigidity under distributed and triangular types of loading. In this analysis, a trigonometric series has been used to express the displacement variation along the nodal lines. In order to simplify the analysis, the variation of plate thickness is considered as a single variable function of the direction perpendicular to the nodal lines. In addition, it is assumed that no abrupt change of the plate thickness occurs in that direction. Although the present formulation is restricted to the trigonometric series fitted the simply supported end conditions, basic functions corresponding to a variety of other boundary conditions could be adopted.

METHOD OF ANALYSIS

a - Nodal line finite difference equation

In deriving the differential equation of equilibrium of rectangular plates with variable thickness, it is assumed that there is no abrupt variation in thickness of the plate. The flexural rigidity B in this case is no longer a constant but a function of the coordinate x and y of the plate surface. The differential equation which represents the equilibrium condition of an element of the plate with variable thickness takes the following form:

$$B(w''''+2w'''+w''') + 2B'(w'''+w'') + 2B''(w''+w'') + (B''+B'')(w''+w'') - (1-\nu)(B''w''-2B'w''+B''w'') = q \quad (1)$$

As a particular application, let us consider the case of elastic isotropic plates in which the flexural rigidity B is a function of x coordinate only and constant in y direction. For this case, equation (1) can be written as follows:

$$B(w''''+2w'''+w''') + 2B'(w'''+w'') + B''(w''+\nu w'') = q \quad (2)$$

where $(\cdot)' = \frac{\partial}{\partial x}$, $(\cdot)'' = \frac{\partial^2}{\partial y^2}$ and

$$B = \frac{E t^3(x)}{12(1-\nu^2)}$$

is the flexural rigidity of the plate with variable thickness in x direction.

Fig. 1 shows some selected different cross-sections for plates having variable thickness in x direction.

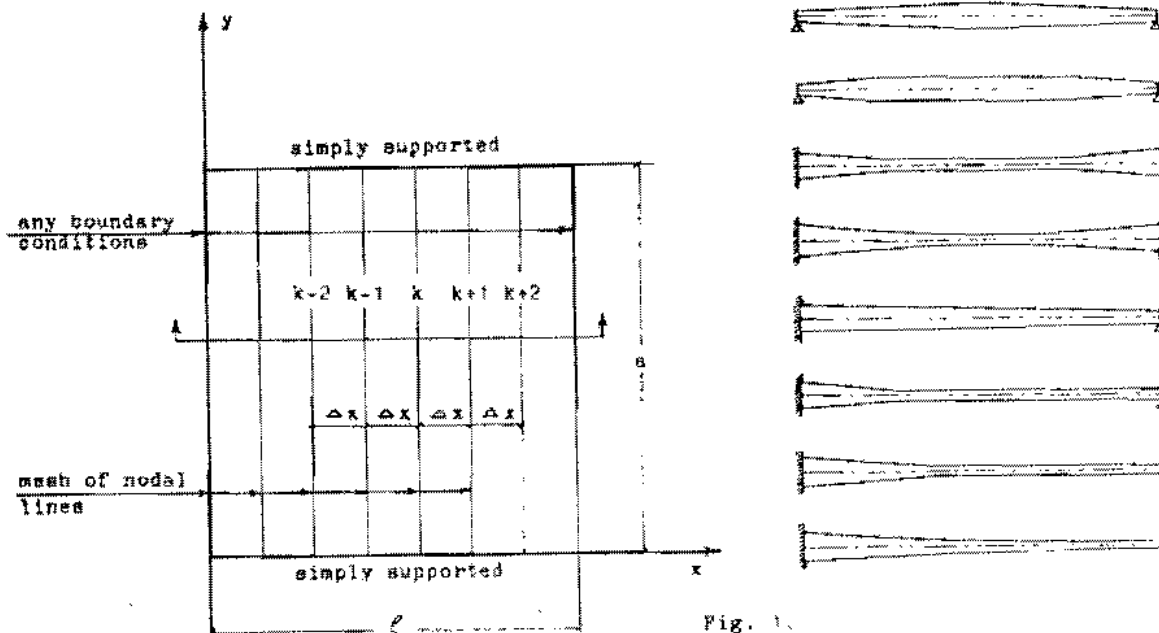


Fig. 1.

In applying the nodal line finite difference method to calculate the deflection and the internal forces in a given rectangular plate with variable thickness, let us begin by dividing the plate into a mesh of fictitious nodal lines as shown in Fig. 1. According to the prescribed boundary conditions of the two opposite ends perpendicular to the nodal lines, a basic function has to be chosen to express the displacement variation along the nodal lines. The displacement function at each nodal line is expressed as a summation of the chosen basic function terms multiplied by a single variable functions as a nodal line parameters. The displacement function at any nodal line labelled k shown in Fig. 1 can be written in the following form

$$w_k = \sum_{m=1}^r f_{m,k}(x) \cdot Y_m(y) \quad (3)$$

Let us restrict our attention here to plates with two opposite simply supported ends perpendicular to the nodal lines. The chosen basic function fitting the boundary conditions at the two ends of the nodal lines is a trigonometric series in the form

$$Y_m(y) = \sin \frac{m\pi}{a} y = \sin k_m y \quad (4)$$

Resolving the load into series similar to that of the chosen basic function and substituting equations (3) and (4) into equation (2) we get

C. 16 YOUSSEF AGAG

$$\sum_{m=1}^r [B_k(f'''' - 2k_m^2 f'' + k_m^4 f'''_m, k) + 2B'_k(f''' - k_m^2 f''_m, k) \\ + B''_k(f'' - k_m^2 f'_m, k)] \sin k_m y = \sum_{m=1}^r q_{m,k} \sin k_m y \quad (5)$$

For each term of the basic function equation (5) takes the form:

$$B_k(f'''' - 2k_m^2 f'' + k_m^4 f'''_m, k) + 2B'_k(f''' - k_m^2 f''_m, k) \\ + B''_k(f'' - k_m^2 f'_m, k) = q_{m,k} \quad (6)$$

By applying the central finite difference technique in the x direction, equation (6) can be written as

$$\frac{1}{\Delta x^4} [C_m^1 f_{m,k-2} + C_m^2 f_{m,k-1} + C_m^3 f_{m,k} + C_m^4 f_{m,k+1} + C_m^5 f_{m,k+2}] = q_{m,k} \quad (7)$$

where $C_m^1 = \frac{1}{2} [\alpha_{k-1} + 2\alpha_k - \alpha_{k+1}]$,
 $C_m^2 = \frac{1}{2} [-\psi_m^2 \alpha_{k-1} - (12 + 4\psi_m^2) \alpha_k + (4 + \psi_m^2) \alpha_{k+1}]$,
 $C_m^3 = [-(2 + \psi_m^2) \alpha_{k-1} + (10 + 4\psi_m^2 + 2\psi_m^2 + \psi_m^4) \alpha_k - (2 + \psi_m^2) \alpha_{k+1}]$,
 $C_m^4 = \frac{1}{2} [(4 + \psi_m^2) \alpha_{k-1} - (12 + 4\psi_m^2) \alpha_k - \psi_m^2 \alpha_{k+1}]$,
 $C_m^5 = \frac{1}{2} [-\alpha_{k-1} + 2\alpha_k + \alpha_{k+1}]$,
 $\psi_m = \frac{k_m a}{\lambda}$, $\lambda = \frac{a}{\Delta x}$, $\alpha_k = \frac{B_k}{B_o}$ and
 $\Delta x = \frac{a}{\lambda}$ is the constant interval between
the nodal lines

Equation (7) can be written in the following form:

$$[C_m^1 \ C_m^2 \ C_m^3 \ C_m^4 \ C_m^5] \{f_{m,k-2} \ f_{m,k-1} \ f_{m,k} \ f_{m,k+1} \ f_{m,k+2}\} \\ = \frac{a^4}{B_o \lambda^4} q_{m,k} \quad (8)$$

Equation (8) represents the central nodal line finite difference equation for the plates of variable flexural rigidity in one direction only (x direction)

Application of equation (8) at each nodal line of the plate gives a system of simultaneous algebraic equations, which can be written in the matrix form as follows:

$$[S1_m \ \{f\}_m] = \{P\}_m \quad (9)$$

where $\{S\}_m$ is a square band matrix,

$\{f\}_m$ is the vector of the unknown nodal line parameters
and $\{P\}_m$ is the load vector.

The square band matrix $[Sl_m]$ whose band width equal 5 can be stored in a rectangular matrix having the dimensions of $M \times 5$. Where M is the number of the nodal lines of the plate.

b - Internal forces

For the elastic isotropic plates having variable thickness in one direction (x direction), the internal forces per unit length at any point are given by

$$\left. \begin{aligned} M_x &= -B(x)(w'' + \gamma w'''') \\ M_y &= -B(x)(w'' + \gamma w''') \\ M_{xy} &= -M_{yx} = B(x)(1-\gamma) w'' \\ Q_x &= -B(x)(w'''' + w''''') \\ Q_y &= -B(x)(w'''' + w''''') \end{aligned} \right\} \quad (10)$$

By applying the central nodal line finite difference technique, the internal forces at any nodal line labelled k can be written in the following form:

$$\left. \begin{aligned} M_{x,k} &= -B_k \frac{\lambda^2}{8a^2} \sum_{m=1}^r [f_{m,k-1} - (2+\gamma\Psi_m^2)f_{m,k} + f_{m,k+1}] \sin k_m y \\ M_{y,k} &= -B_k \frac{\lambda^2}{8a^2} \sum_{m=1}^r [\gamma f_{m,k-1} - (2\gamma+\Psi_m^2)f_{m,k} + \gamma f_{m,k+1}] \sin k_m y \\ M_{xy,k} &= B_k \frac{\lambda^2}{2a^2} (1-\gamma) \sum_{m=1}^r \Psi_m [f_{m,k-1} - f_{m,k} + f_{m,k+1}] \cos k_m y \\ Q_{x,k} &= -B_k \frac{\lambda^3}{2a^3} \sum_{m=1}^r [-f_{m,k-2} + (2+\Psi_m^2)f_{m,k-1} - (2+\Psi_m^2)f_{m,k+1} \\ &\quad + f_{m,k+2}] \sin k_m y \\ Q_{y,k} &= -B_k \frac{\lambda^3}{2a^3} \sum_{m=1}^r \Psi_m [f_{m,k-1} - (2+\Psi_m^2)f_{m,k} + f_{m,k+1}] \cos k_m y \end{aligned} \right\} \quad (11)$$

c - Boundary conditions

The boundary conditions are the conditions at the edges which must be prescribed in advance in order to obtain the solution of a specific plate bending problem. The application of the nodal line finite difference method in the analysis of rectangular plates in bending requires the division of the plate into a mesh of parallel nodal lines. The two opposite ends perpendicular to the nodal lines control the choice of the basic function described the displacement variation along the nodal lines. The other two opposite ends can take any combination of boundary conditions.

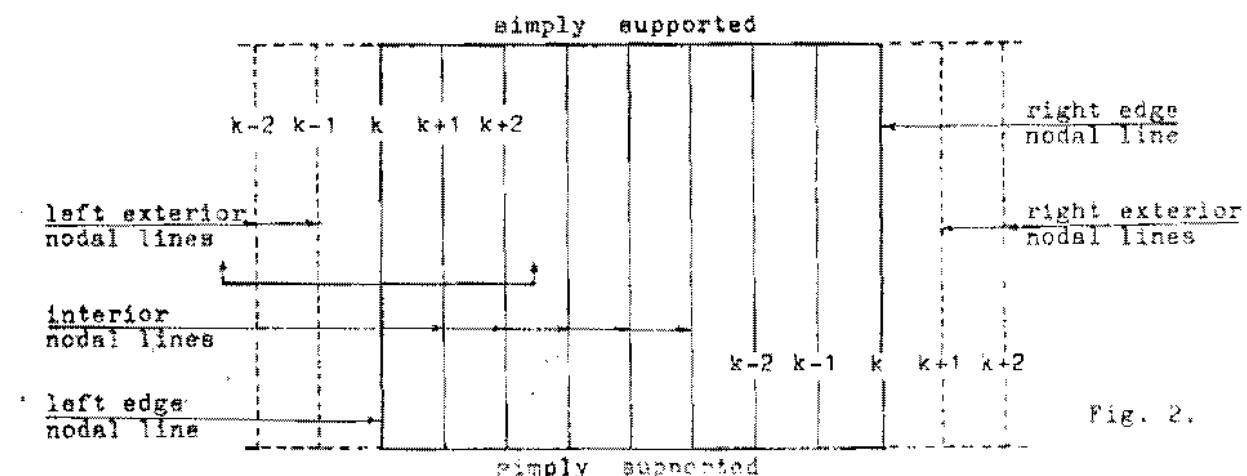
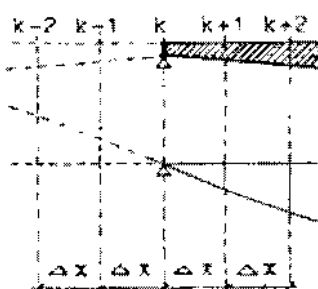


Fig. 2.

The analysis of plate bending problems via the proposed technique requires the application of the central nodal line finite difference equation at each nodal line within the plate including the edge nodal lines. If the pivotal nodal line k is at the left or the right edge (fig. 2), two fictitious nodal lines outside the plate must be introduced. According to the prescribed boundary conditions at the edge nodal lines, the parameters of the exterior nodal lines have to be expressed in terms of the edge and the two adjacent interior nodal lines. Thus the parameters of the exterior nodal lines can be written in the following form:

$$1 - \text{Simply supported edge } [w_k = 0 , (w'' + \gamma w'')_k = 0]$$

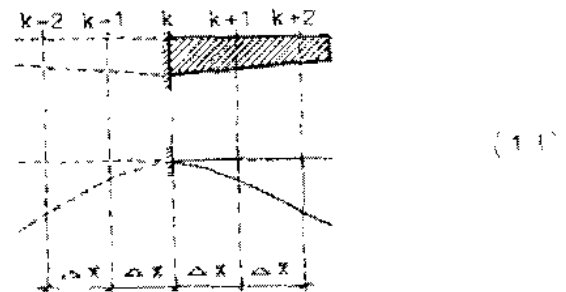
$$\left. \begin{aligned} f_{m,k} &= 0 \\ f_{m,k-1} &= -f_{m,k+1} \\ f_{m,k-2} &= -f_{m,k+2} \end{aligned} \right\}$$



(12)

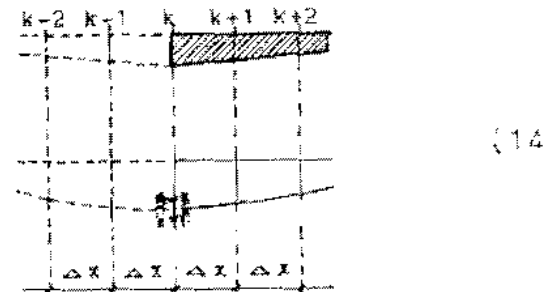
2 - Clamped edge [$w_k = 0$, $w'_k = 0$]

$$\left. \begin{array}{l} f_{m,k} = 0 \\ f_{m,k-1} = f_{m,k+1} \\ f_{m,k-2} = f_{m,k+2} \end{array} \right\}$$



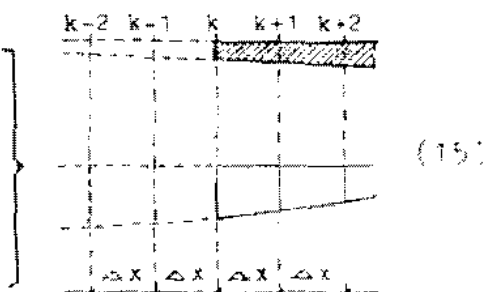
3 - Guided edge [$w_k = 0$, $\{ w''' + w'''\}_k = 0$]

$$\left. \begin{array}{l} f_{m,k} \neq 0 \\ f_{m,k-1} = f_{m,k+1} \\ f_{m,k-2} = f_{m,k+2} \end{array} \right\}$$



4 - Free edge [$\{ w''' + \gamma w'''\}_k = 0$, $\{ w''' + (2-\gamma) w'''\}_k = 0$]

$$\left. \begin{array}{l} f_{m,k} \neq 0 \\ f_{m,k-1} = \bar{\Sigma}_1 f_{m,k} - f_{m,k+1} \\ f_{m,k-2} = \bar{\Sigma}_2 f_{m,k} - 2 \bar{\Sigma}_1 f_{m,k+1} + f_{m,k+2} \end{array} \right\}$$



where

$$\bar{\Sigma}_1 = (2+\gamma \psi_m^2) , \quad \bar{\Sigma}_2 = [2+(2-\gamma) \psi_m^2]$$

C. 20 YOUSSEF AGAG
NUMERICAL EXAMPLES

The proposed technique has been used to analyze thin elastic isotropic rectangular plates having variable flexural rigidity in one direction. Two opposite sides of each plate are considered as simply supported, while the other two sides can take any combination of boundary conditions. Four examples have been selected to demonstrate the efficiency of the proposed technique. Only the odd terms of the basic function are used because of symmetry in direction of the nodal lines. Informations regarding boundary conditions, type of loading and variation of thickness of the plate are illustrated in Figs. 3 and 4.

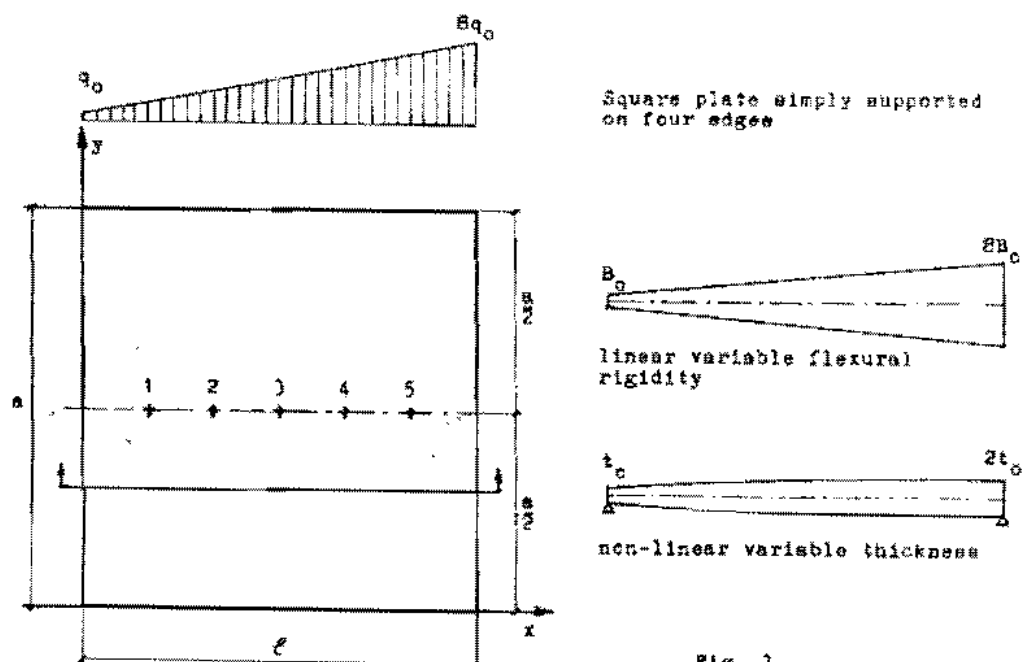


Fig. 3.

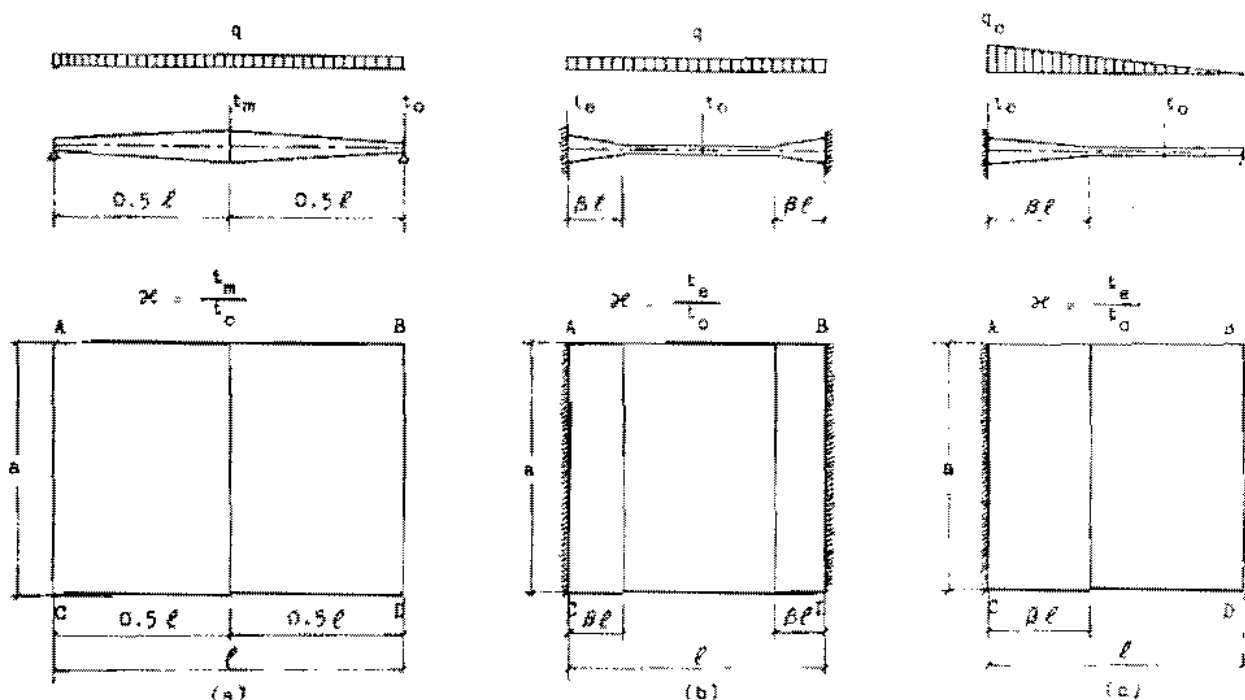


Fig. 4.

† - Analysis of square plate simply supported on four sides subjected to trapezoidal distributed load. Fig. 3.
(No. of terms = 1 - 3 - 5 - 7, $\Delta x = \ell/24$, $\ell/a = 1$, $\nu = 0.16$)

Square plate with linear variable flexural rigidity has been analyzed. The plate is divided into a mesh of twenty five nodal lines i.e. $\Delta x = \ell/24$. The analysis is carried out for selected number of terms of the basic function. The results obtained are summarized in Table I. Comparison is done with those of the finite strip, the finite element and the exact solution results presented in Table 5 (REFERENCE [2]). The results demonstrate a close agreement with these known solutions.

Table I. Square plate with linear variable flexural rigidity simply supported on four sides under trapezoidal distributed load (Fig. 3)

Poisson's ratio $\nu = 0.16$	Point	Source : Proposed Technique				Source : Table 5 Reference [2]		
		Nodal Line Finite Difference $\Delta x = \ell/24$, 25 Nodal Lines 25 Equations				Finite Strip	Finite Element	Exact
		No. of Terms				$m = 1$ 26 Equations	72 Elements 273 Equations	
$w \cdot \frac{\pi^5 B_0}{4 q_0 a^4}$	1	0.1994	0.1968	0.1957	0.1967	0.1991	0.1964	0.1996
	2	0.3080	0.3045	0.3045	0.3045	0.3079	0.3043	0.3106
	3	0.3271	0.3235	0.3235	0.3235	0.3272	0.3234	0.3264
	4	0.2710	0.2678	0.2677	0.2677	0.2712	0.2676	0.2724
	5	0.1549	0.1527	0.1526	0.1526	0.1550	0.1525	0.1553
$M_x \cdot \frac{\pi^3}{4 q_0 a^2}$	1	0.836	0.815	0.814	0.814	0.836	0.759	0.837
	2	1.265	1.242	1.241	1.241	1.259	1.233	1.265
	3	1.478	1.452	1.451	1.450	1.470	1.442	1.483
	4	1.507	1.469	1.468	1.468	1.502	1.455	1.500
	5	1.180	1.129	1.126	1.126	1.189	1.103	1.139
$M_y \cdot \frac{\pi^3}{4 q_0 a^2}$	1	0.559	0.516	0.513	0.512	0.497	0.502	0.563
	2	1.209	1.121	1.116	1.115	1.114	1.099	1.212
	3	1.677	1.555	1.548	1.547	1.577	1.526	1.673
	4	1.744	1.604	1.596	1.594	1.660	1.573	1.478
	5	1.226	1.112	1.103	1.101	1.178	1.083	1.291

2 - Analysis of rectangular plates simply supported on four sides subjected to uniform load of intensity q . Fig. 4-a
(No. of terms = 7, $\Delta x = \ell/40$, $\Delta l = t_m/t_o$, $\lambda = \ell/a$, $\nu = 0.3$)

Rectangular plates with different ratios of rectangularity λ and thickness ratios Δl have been analyzed. The analysis deals with the effect of thickness ratios Δl on the deflection and the internal forces of the plate. Due to symmetry, only half of the plate (divided into twenty one nodal lines i.e. $\Delta x = \ell/40$) is considered in the analysis. Regarding the central point of the plate, results are presented in a form of numerical factors in Tables 1, 2 and 3 (APPENDIX I). These numerical factors are plotted in curves shown in Figs. 5-a, 5-b and 5-c.

C. 22 YOUSSEF AGAB

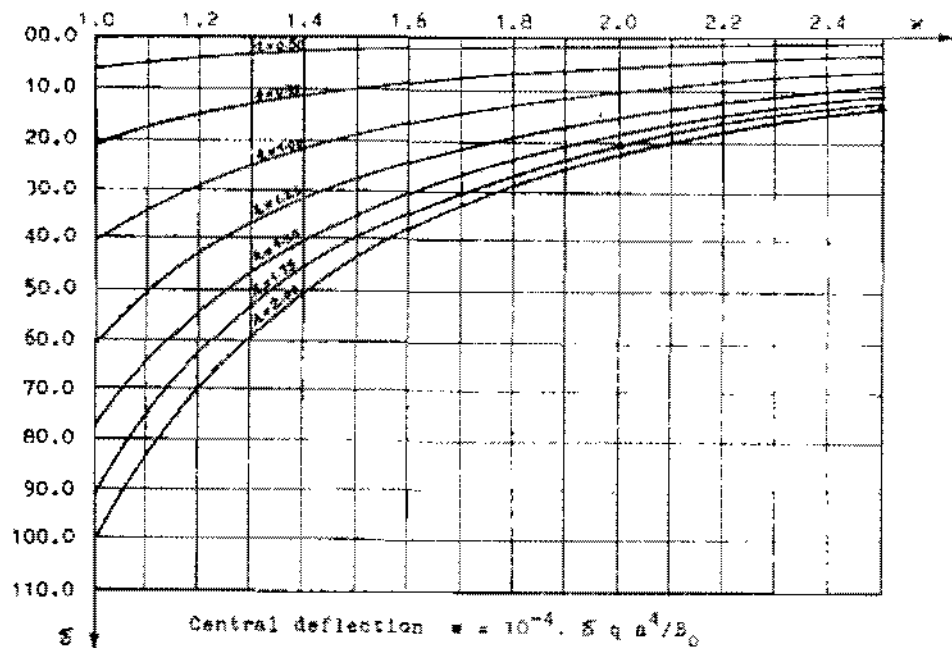


Table 1.

Fig. 5-a

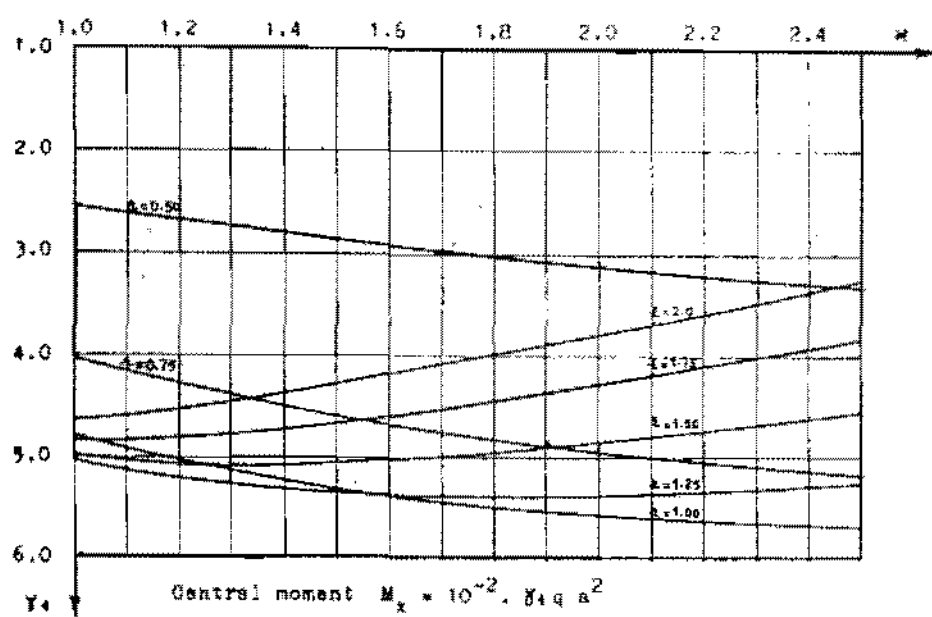


Table 2.

Fig. 5-b

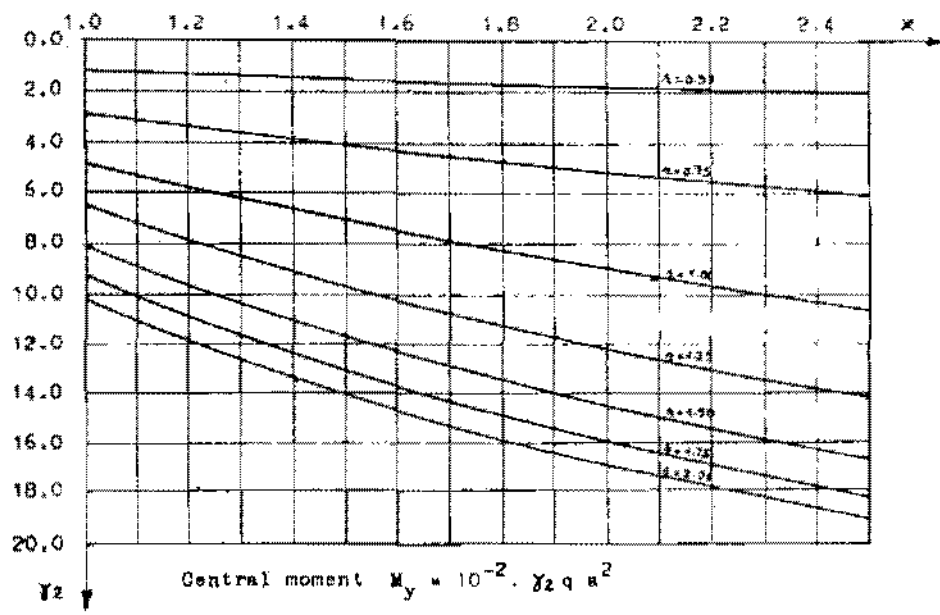


Table 3.

Fig. 5-c

The curves show decrease of the central deflection and increase of the central moment M_y with the increase of the thickness ratio $\beta\ell$ (for different ratios of rectangularity β) as expected. It should be mentioned that, while the central moment M_x increases with the increase of the thickness ratio $\beta\ell$ for the ratios of rectangularity $\beta \leq 1$, it decreases for the ratios of rectangularity $\beta > 1$.

- 3 - Analysis of square plates clamped on sides AC and BD, simply supported on the other two sides subjected to uniform load of intensity q . Fig. 4-b.
 (No. of terms = 7, $\Delta x = \ell/100$, $\beta\ell = t_e/t_o$, $\nu = 0.3$)

Square plates having haunches with increased thickness toward the clamped edges have been analyzed. The analysis aims at the study of the effect of thickness ratio $\beta\ell$ and length ratio β of haunches on the deflection and the internal forces of the plate. The analysis was performed for half of the plate (divided into a fine mesh of fifty one nodal lines i.e. $\Delta x = \ell/100$) because of symmetry. The results were obtained in a form of numerical factors especially for the central point of the plate and the middle point of the clamped edges. These factors are given in Tables 4, 5, 6 and 7 (APPENDIX I). Moreover these numerical factors are plotted against the thickness ratio $\beta\ell$ for different length ratios β in a form of curves shown in Figs. 6-a, 6-b, 6-c and 6-d.

An inspection of Fig. 6-a leads to the conclusion that, the increase of either the thickness ratio $\beta\ell$ or the length ratio β of the haunch decreases the deflection at the central point of the plate. It can also be concluded that, the central moment M_x and M_y decrease against increasing the thickness ratio $\beta\ell$. On the other hand, increasing the length ratio β may decrease or increase the central moment M_x and M_y . This is clearly illustrated in the disarrangement of the length ratio curves ($0 < \beta \leq 0.5$) given in Figs. 6-b and 6-c.

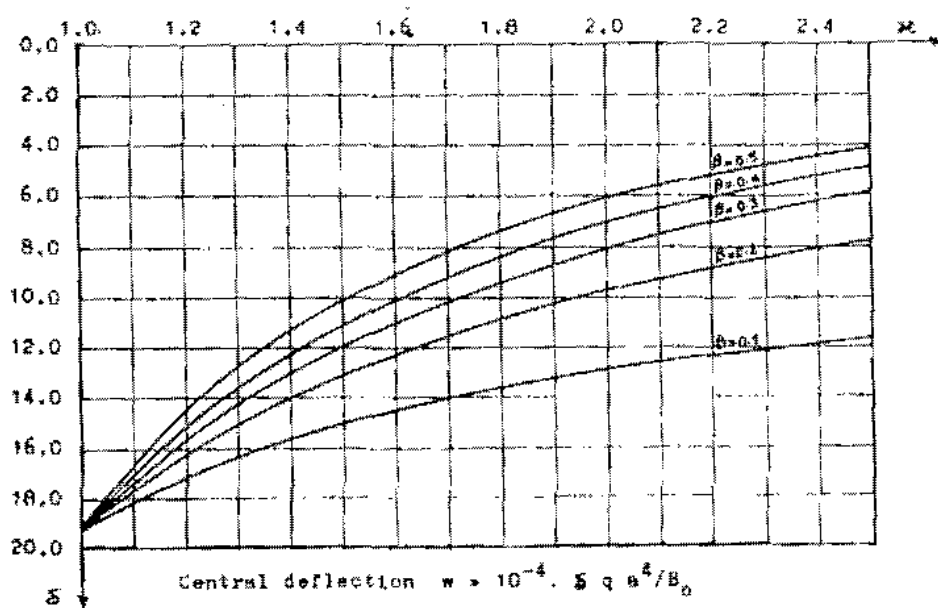


Table 4.

Fig. 6-a

C. 24 YOUSSEF AGAG

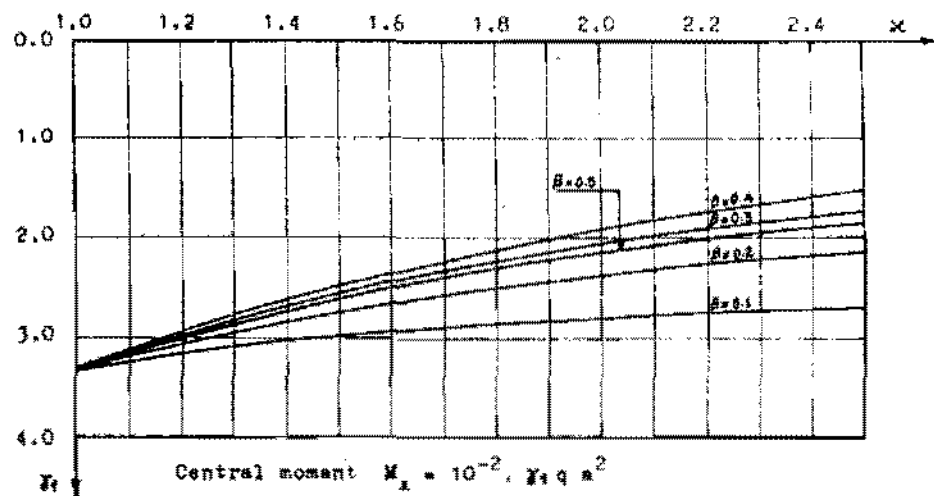


Table 5.

Fig. 6-b

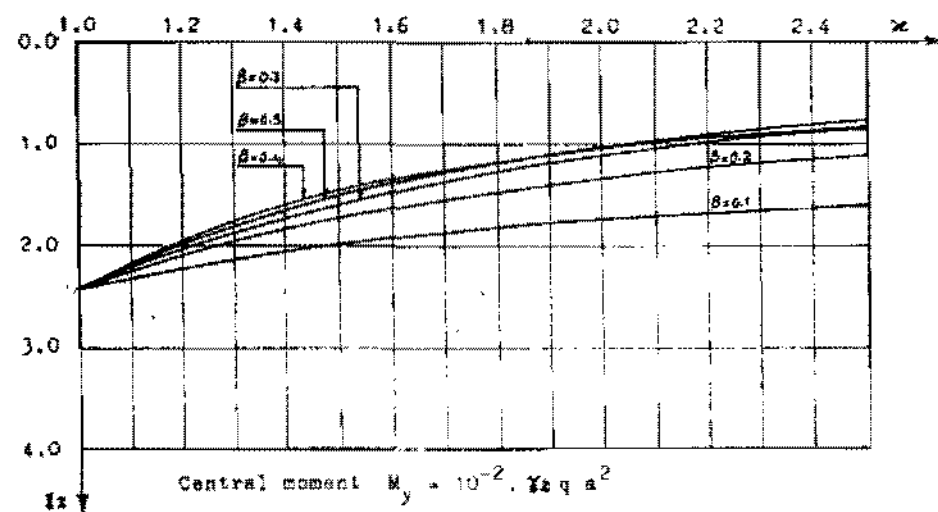


Table 6.

Fig. 6-c

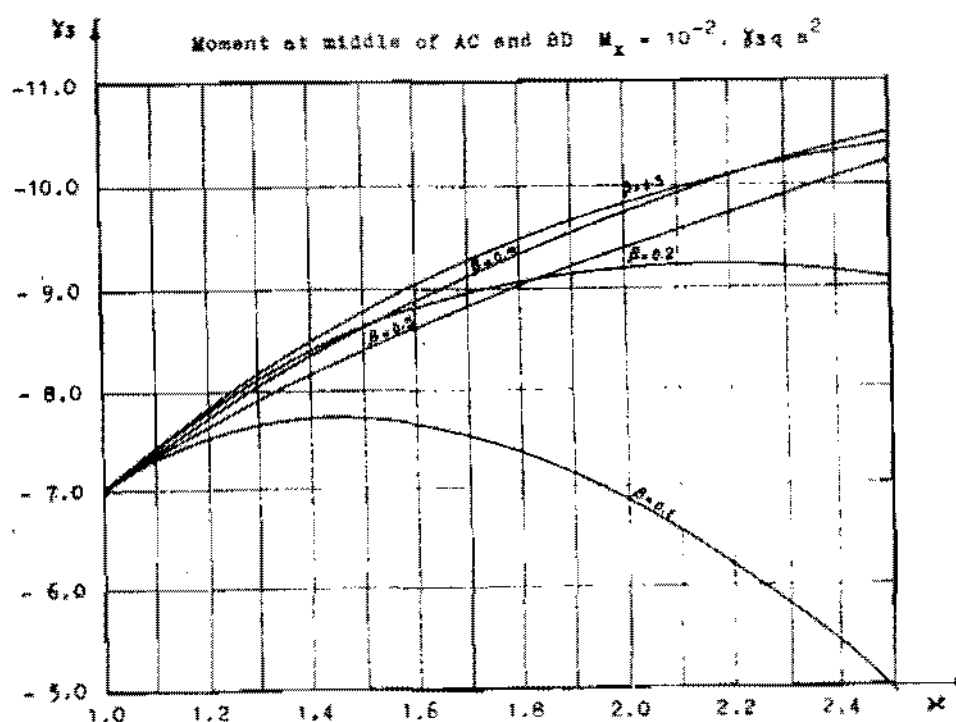


Table 7.

Fig. 6-d

The increase of the thickness ratio α of the haunch increases the fixation moment M_x at the clamped edges. Fig. 6-d shows that, for each length ratio β there is an optimal thickness ratio α at which the maximum value of the moment M_x at the middle point of the clamped edges is occurred. Any value for the thickness ratio α beyond the optimal one will decrease the resultant moment M_x . This is due to the rapid decrease of the deflection of the plate at the neighbourhood of the clamped edges.

- 4 - Analysis of square plates clamped on side AC, simply supported on the other three sides subjected to triangular distributed load. Fig. 4-c
(NQ. of terms = 7 , $\Delta x = \ell/50$, $\alpha = t_e/t_o$, $\nu = 0.3$)

Square plates with one haunch at the clamped edge under triangular distributed load have been analyzed. The analysis is performed to study the effect of the haunch on the deflection and the internal forces of the plate. In this analysis, the plate is divided into a mesh of fifty one nodal lines ($\Delta x = \ell/50$). The results obtained are presented in a form of numerical factors for central point of the plate and middle point of the clamped edge. These results are summarized in the Tables 8,9,10 and 11 (APPENDIX I). In addition, plotting of these numerical factors against the thickness ratio α of the haunch are illustrated in Figs. 7-a, 7-b, 7-c and 7-d.

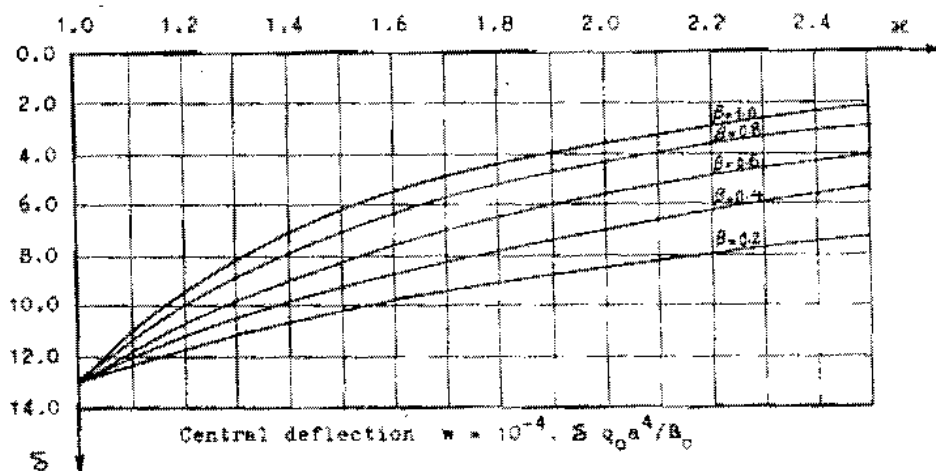


Table 8.

Fig. 7-a

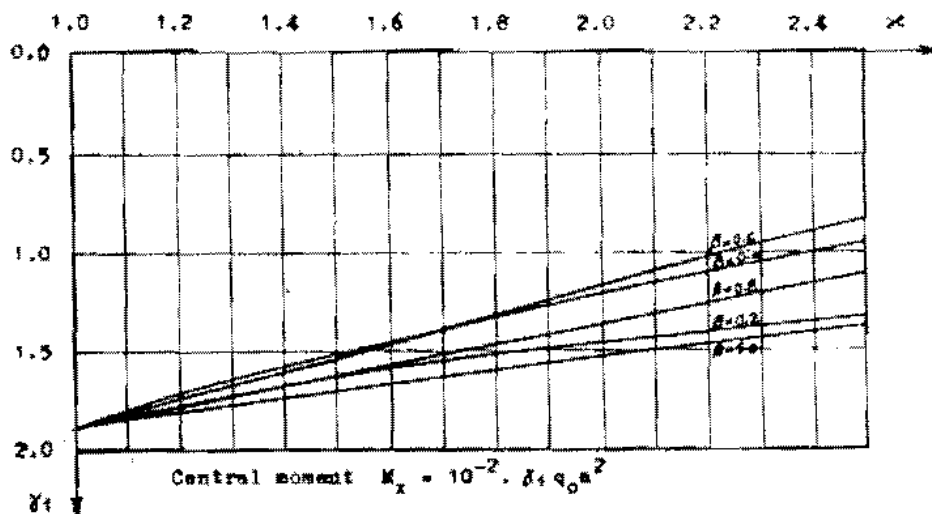


Table 9.

Fig. 7-b

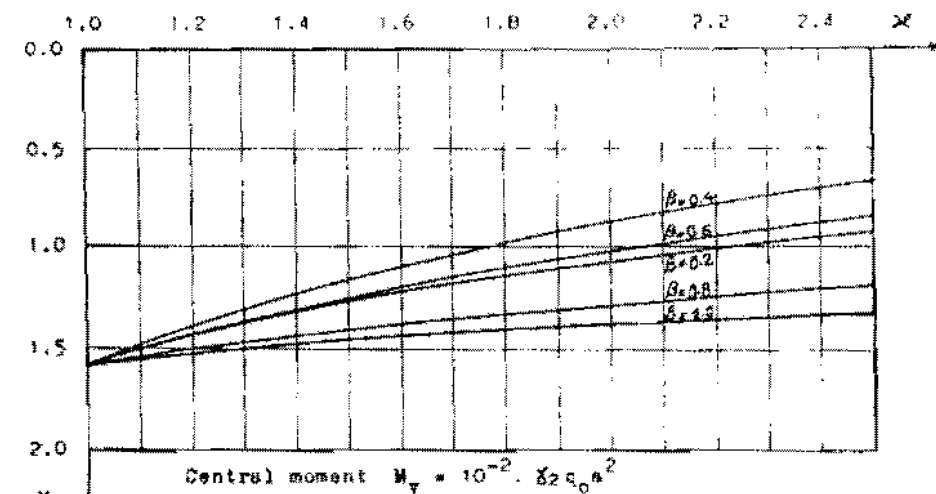


Table 10.

Fig. 7-c

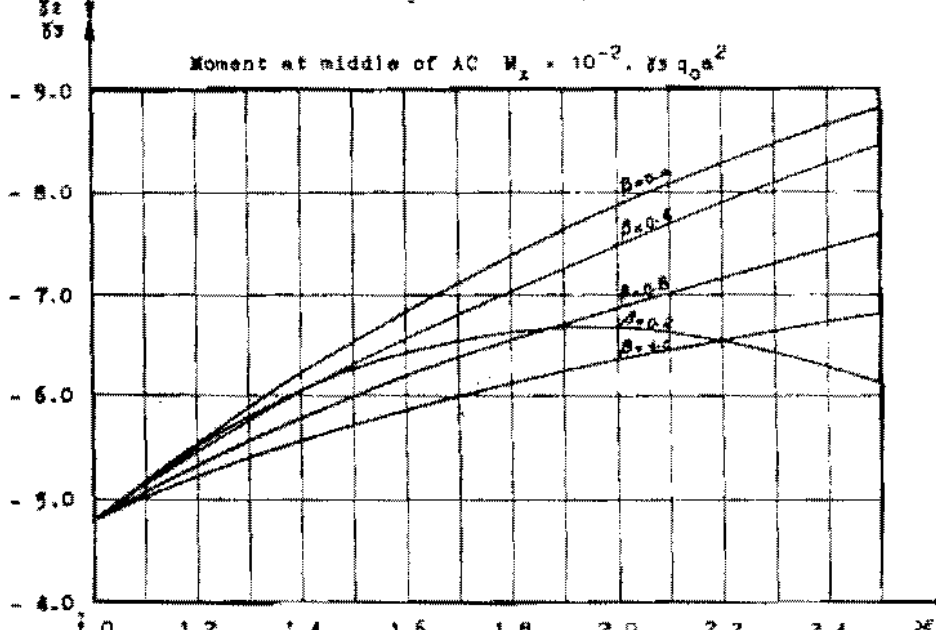


Table 11.

Fig. 7-d

A close study of Figs. 7-a, 7-b, 7-c and 7-d reveal that the haunch effect considered in the present example is similar to the one in the third example. Therefore, similar conclusions can be drawn.

CONCLUSION

The importance of the nodal line finite difference method presented herein, lies in the ease with which it can be applied to bending problems of rectangular plates with variable flexural rigidity. Using this method, it enables one to overcome the mathematical complexities of the solution of these types of problems. Four examples have been selected to demonstrate the efficiency of the proposed technique. A problem for which known solutions are available, is presented in the first example. This problem was selected so that a comparison between these known solutions and the proposed one can be done. The results obtained demonstrate a close agreement with the available solutions. The other three examples aim at the study of the effect of the plate thickness variation on the structural behaviour of the plate. The results indicate the considerable effect of plate thickness variation on the deflection and the internal forces.

APPENDIX I

Tables of numerical factors for deflection and bending moments

1 - Rectangular plate simply supported on all sides Fig. 4-a

Table 1. Numerical factor ξ for central deflection w

$\frac{A}{x}$	0.50	0.75	1.00	1.25	1.50	1.75	2.00	
1.0	6.33		40.60		77.20		101.10	Exact (6)
1.0	6.3225	20.9769	40.6223	60.2607	77.2202	90.8029	101.2486	N.L.P.D.
1.1	5.2035	17.6621	34.2914	50.6787	64.5570	75.4211	83.5652	"
1.2	4.4765	15.0970	29.2801	43.0562	54.5872	62.3960	69.8447	"
1.3	3.8452	13.0782	25.2448	36.9990	46.6121	53.8402	59.0192	"
1.4	3.3358	11.0455	21.9489	32.0285	40.1456	46.1399	50.3429	"
1.5	2.9521	9.9381	19.2240	27.9319	34.8406	39.8590	43.3092	"
1.6	2.5709	8.8066	16.9474	24.5187	30.4435	34.8610	37.5466	"
1.7	2.2916	7.8253	15.0278	21.6499	26.7654	30.7715	32.7623	"
1.8	2.0486	6.9960	13.3959	19.2183	23.6634	26.1529	28.7587	"
1.9	1.8412	6.2654	11.9984	17.1450	21.0278	23.6931	25.4038	"
2.0	1.6627	5.6721	10.7936	15.3531	18.7732	21.0866	22.5481	"
2.1	1.5081	5.1354	9.7467	13.8232	16.827	18.8513	20.1079	"
2.2	1.3732	4.6741	8.6375	12.4650	15.1529	16.9234	18.0959	"
2.3	1.2549	4.2655	8.0389	11.3162	13.5913	15.2514	16.1955	"
2.4	1.1506	3.9049	7.3356	10.2905	12.4112	13.7940	14.6191	"
2.5	1.0682	3.5852	6.7136	9.3865	11.2905	12.5170	13.2410	"

$$w = 10^{-4} \cdot \xi \cdot q \cdot a^4 / h_0$$

Table 2. Numerical factor η_1 for central moment M_x

$\frac{A}{x}$	0.50	0.75	1.00	1.25	1.50	1.75	2.00	
1.0	2.34		4.79		4.98		4.64	Exact (6)
1.0	2.3424	4.0215	4.7875	5.0250	4.9833	4.8245	4.6348	N.L.P.D.
1.1	2.0641	4.1493	4.9865	5.1275	5.0312	4.9193	4.5864	"
1.2	2.6677	4.2696	5.0495	5.2053	5.0590	4.7968	4.5229	"
1.3	2.1309	4.3816	5.1574	5.2744	5.0684	4.7588	4.4415	"
1.4	2.7925	4.4850	5.2511	5.3228	5.0651	4.7087	4.3628	"
1.5	2.0520	4.5801	5.3320	5.3574	5.0483	4.6486	4.2732	"
1.6	2.3090	4.6674	5.4013	5.3799	5.0212	4.5811	4.1744	"
1.7	2.5634	4.7474	5.4601	5.3919	4.9855	4.5024	4.0739	"
1.8	3.0151	4.8205	5.5057	5.3850	4.9428	4.4290	3.9709	"
1.9	3.0641	4.8832	5.5510	5.3903	4.8943	4.3470	3.8663	"
2.0	3.1106	4.9481	5.5849	5.3790	4.8412	4.2625	3.7611	"
2.1	3.1546	5.0035	5.6122	5.3621	4.7842	4.1762	3.6546	"
2.2	3.1952	5.0541	5.6336	5.3402	4.7243	4.0888	3.5505	"
2.3	3.2355	5.1000	5.6498	5.3143	4.6626	4.0007	3.4461	"
2.4	3.2727	5.1417	5.6614	5.2848	4.5975	3.9123	3.3427	"
2.5	3.3079	5.1796	5.6687	5.2723	4.5325	3.8241	3.2405	"

$$\eta_1 = 10^{-2} \cdot \xi \cdot q \cdot a^2$$

Table 3. Numerical factor η_2 for central moment M_y

$\frac{A}{x}$	0.50	0.75	1.00	1.25	1.50	1.75	2.00	
1.0	3.16		4.79		6.12		10.17	Exact (6)
1.0	3.1611	2.8336	4.7903	6.6108	8.1160	9.2664	10.1669	N.L.P.D.
1.1	3.2220	3.0764	5.2591	7.2656	8.8942	10.1299	11.0348	"
1.2	3.2946	3.3178	5.7187	7.9024	9.6407	10.9320	11.8537	"
1.3	3.3480	3.5358	6.1674	8.3163	10.3346	11.8927	12.8253	"
1.4	3.4115	3.7915	6.6042	9.1072	11.0159	12.4135	13.3921	"
1.5	3.4749	4.0223	7.0283	9.6757	11.5854	13.0959	14.0366	"
1.6	3.5376	4.2484	7.4396	10.2214	12.3062	13.7422	14.6813	"
1.7	3.6001	4.4698	7.8379	10.7452	12.8936	14.3544	15.2803	"
1.8	3.5517	4.6862	8.2235	11.2477	13.4552	14.9346	15.8648	"
1.9	3.7224	4.8976	8.5965	11.7251	13.9904	15.4950	16.4079	"
2.0	3.7823	5.1040	8.9574	12.1922	14.5007	16.0074	16.9210	"
2.1	3.8412	5.3054	9.3064	12.6361	14.9876	16.5039	17.4008	"
2.2	3.8992	5.3020	9.6440	13.0622	15.4525	16.9760	17.8707	"
2.3	3.9563	5.6937	9.9706	13.4714	15.8967	17.4056	18.3053	"
2.4	2.0123	5.8808	10.2866	13.8637	16.0214	17.8540	18.7264	"
2.5	3.0674	6.0633	10.5924	14.2428	16.7277	18.2626	19.1335	"

$$\eta_2 = 10^{-2} \cdot \xi \cdot q \cdot a^2$$

C. 23 YOUSSEF AGAG

2 - Square plate clamped on two opposite sides, simply supported on the other two opposite sides Fig. 4-b

Table 4. Numerical factor δ for central deflection w

$\frac{\beta}{\pi}$	0.1	0.2	0.3	0.4	0.5	
1.0	19.20	19.20	19.20	19.20	19.20	
1.0	19.1843	19.1843	19.1843	19.1843	19.1843	Exact 161
1.1	18.1131	17.6126	17.2998	16.9334	16.5923	X.L.P.D.
1.2	17.1938	16.2459	15.6757	15.1503	14.4811	
1.3	16.3902	15.0537	14.2638	13.3840	12.1799	
1.4	15.7045	14.0045	13.0345	12.2412	11.2882	
1.5	15.0960	13.0785	11.9515	11.0810	10.0661	
1.6	14.5592	12.2574	10.9554	10.0715	9.0284	
1.7	14.0833	11.5261	10.1470	9.1880	8.1405	
1.8	13.6597	10.8720	9.1910	8.4101	7.3754	
1.9	13.3810	10.2857	8.7147	7.7218	6.7118	
2.0	12.9414	9.7575	8.1074	7.1101	6.1331	
2.1	12.5359	9.2866	7.5604	6.5540	6.6256	
2.2	12.3604	8.8485	7.0661	6.0746	5.1784	
2.3	12.1111	8.4561	6.6181	5.6344	4.7825	
2.4	11.8852	8.0982	6.2110	5.2272	4.3307	
2.5	11.6800	7.7725	5.8401	4.8777	4.1168	

$$* \times 10^{-4}, S \cdot g \cdot m^2/B_a$$

Table 5. Numerical factor γ_1 for central moment M_x

$\frac{\beta}{\pi}$	0.1	0.2	0.3	0.4	0.5	
1.0	3.32	3.32	3.32	3.32	3.32	
1.0	3.3254	3.3254	3.3254	3.3254	3.3254	Exact 161
1.1	3.3288	3.1818	3.1454	3.1012	3.0496	X.L.P.D.
1.2	3.1613	3.0277	2.9803	2.9516	2.9905	
1.3	3.0972	2.9364	2.8299	2.7857	2.8464	
1.4	3.0389	2.8315	2.6902	2.6325	2.7158	
1.5	2.9871	2.7367	2.5570	2.4599	2.5571	
1.6	2.9410	2.6507	2.4462	2.3600	2.4492	
1.7	2.8997	2.5726	2.3368	2.2088	2.3909	
1.8	2.8626	2.5013	2.2299	2.1266	2.2012	
1.9	2.8291	2.4363	2.1409	2.0224	2.2193	
2.0	2.7989	2.3768	2.0647	1.9257	2.1443	
2.1	2.7714	2.3222	1.9869	1.8357	2.0757	
2.2	2.7464	2.2719	1.9149	1.7519	2.0128	
2.3	2.7236	2.2257	1.8481	1.6718	1.9551	
2.4	2.7028	2.1829	1.7860	1.6008	1.8021	
2.5	2.6838	2.1434	1.7283	1.5266	1.6536	

$$M_x = 10^{-2}, S \cdot g \cdot m^2$$

Table 6. Numerical factor γ_2 for central moment M_y

$\frac{\beta}{\pi}$	0.1	0.2	0.3	0.4	0.5	
1.0	2.44	2.44	2.44	2.44	2.44	
1.0	2.4422	2.4422	2.4422	2.4422	2.4422	Exact 161
1.1	2.3223	2.2621	2.2263	2.2002	2.1787	X.L.P.D.
1.2	2.2193	2.1047	2.0379	1.9797	1.9609	
1.3	2.1101	1.9664	1.8725	1.8136	1.7787	
1.4	2.0522	1.8644	1.7266	1.6079	1.6247	
1.5	1.9839	1.7363	1.5912	1.5204	1.4934	
1.6	1.9237	1.6402	1.4820	1.3995	1.3805	
1.7	1.8702	1.5540	1.3780	1.2924	1.2627	
1.8	1.8227	1.4734	1.2868	1.1968	1.1575	
1.9	1.7802	1.4083	1.2038	1.1113	1.1228	
2.0	1.7421	1.3459	1.1289	1.0345	1.0569	
2.1	1.7078	1.2896	1.0611	0.9652	0.9981	
2.2	1.6770	1.2385	0.9997	0.9025	0.9469	
2.3	1.6490	1.1921	0.9438	0.8457	0.9007	
2.4	1.6237	1.1439	0.8923	0.7939	0.8533	
2.5	1.6006	1.1113	0.8464	0.7466	0.8222	

$$M_y = 10^{-2}, S \cdot g \cdot m^2$$

Table 7. Numerical factor γ_3 for moment M_z at middle of AC and BC

$\frac{\beta}{\pi}$	0.1	0.2	0.3	0.4	0.5	
1.0	-6.97	-6.97	-6.97	-6.97	-6.97	
1.0	-6.9832	-6.9832	-6.9832	-6.9832	-6.9832	Exact 161
1.1	-7.2797	-7.4013	-7.4104	-7.3706	-7.3100	X.L.P.D.
1.2	-7.1977	-7.3602	-7.2891	-7.2557	-7.2609	
1.3	-7.6402	-8.0866	-8.1523	-8.0580	-7.8044	
1.4	-7.7108	-8.3994	-8.4721	-8.1324	-8.1398	
1.5	-7.7734	-8.5895	-8.7616	-8.5295	-8.3781	
1.6	-7.8524	-8.7795	-9.0220	-8.8854	-8.6017	
1.7	-7.5319	-8.9320	-9.2560	-9.1230	-8.8126	
1.8	-7.3565	-9.0454	-9.4659	-9.3410	-9.0125	
1.9	-7.1305	-9.1339	-9.6527	-9.5440	-9.2039	
2.0	-6.8580	-9.1816	-9.8187	-9.7321	-9.3850	
2.1	-6.5442	-9.2126	-9.9636	-9.9066	-9.5600	
2.2	-6.1924	-9.2107	-10.0906	-10.0665	-9.7287	
2.3	-5.8069	-9.1835	-10.2002	-10.2107	-9.8922	
2.4	-5.3918	-9.1327	-10.2926	-10.3581	-10.0511	
2.5	-4.5509	-9.0599	-10.3718	-10.4874	-10.2062	

$$M_z = 10^{-2}, S \cdot g \cdot m^2$$

3 - Square plate clamped on one side, simply supported on the other three sides Fig. 4-c

Table 8. Numerical factor ξ_2 for central deflection w

$\frac{x}{R}$	0.2	0.4	0.6	0.8	1.0	
1.0	13.00	13.00	13.00	13.00	13.00	Exact (6)
1.0	12.8644	12.8644	12.8644	12.8644	12.8644	E.L.P.D.
1.1	12.2146	11.9636	11.6731	11.2349	10.9212	*
1.2	11.6291	11.1640	10.5229	9.8865	9.3702	*
1.3	11.0979	10.4477	9.5184	8.7585	8.1025	*
1.4	10.6136	9.8013	8.8120	7.8051	7.0588	*
1.5	10.1704	9.2142	8.1055	6.9948	6.1907	*
1.6	9.7634	8.6781	7.4802	6.2979	5.4622	*
1.7	9.3868	8.1882	6.9241	5.6956	4.8458	*
1.8	9.0432	7.7231	6.4268	5.1721	4.2205	*
1.9	8.7238	7.3143	5.9800	4.7143	3.6598	*
2.0	8.4264	6.9256	5.5767	4.3118	3.4808	*
2.1	8.1348	6.3647	5.2113	3.9562	3.1430	*
2.2	7.9012	6.2280	4.8788	3.6408	2.8483	*
2.3	7.6659	5.9136	4.5754	3.3597	2.5899	*
2.4	7.4476	5.6196	4.2376	3.1083	2.3622	*
2.5	7.2449	5.3437	4.0425	2.8827	2.1609	*

$$\ast = 10^{-4} \cdot \delta q_0 R^4 / B_0$$

Table 9. Numerical factor ξ_1 for central moment M_x

$\frac{x}{R}$	0.2	0.4	0.6	0.8	1.0	
1.0	1.90	1.90	1.90	1.90	1.90	Exact (6)
1.0	1.8850	1.8850	1.8850	1.8850	1.8850	E.L.P.D.
1.1	1.8287	1.8066	1.8185	1.8405	1.8526	*
1.2	1.7763	1.7339	1.7485	1.7921	1.8181	*
1.3	1.7275	1.6508	1.6765	1.7410	1.7826	*
1.4	1.6819	1.5699	1.6033	1.6803	1.7466	*
1.5	1.6393	1.5211	1.5297	1.6346	1.7108	*
1.6	1.5994	1.4546	1.4562	1.5808	1.6793	*
1.7	1.5619	1.3903	1.3832	1.5257	1.6404	*
1.8	1.5269	1.3282	1.3108	1.4729	1.6061	*
1.9	1.4940	1.2683	1.2394	1.4193	1.5730	*
2.0	1.4631	1.2105	1.1690	1.3662	1.5405	*
2.1	1.4341	1.1548	1.0998	1.2138	1.5090	*
2.2	1.4069	1.1012	1.0319	1.2620	1.4784	*
2.3	1.3814	1.0495	0.9853	1.2109	1.4487	*
2.4	1.3574	0.9997	0.9001	1.1603	1.4199	*
2.5	1.3349	0.9517	0.8362	1.1109	1.3919	*

$$M_x = 10^{-2} \cdot \delta q_0 R^2$$

Table 10. Numerical factor ξ_2 for moment M_y

$\frac{x}{R}$	0.2	0.4	0.6	0.8	1.0	
1.0	1.60	1.60	1.60	1.60	1.60	Exact (6)
1.0	1.5799	1.5799	1.5799	1.5799	1.5799	E.L.P.D.
1.1	1.5062	1.4803	1.5040	1.5395	1.5520	*
1.2	1.4393	1.3699	1.3437	1.3024	1.3265	*
1.3	1.3783	1.3072	1.3709	1.4660	1.5032	*
1.4	1.3284	1.2313	1.3119	1.4360	1.4816	*
1.5	1.2710	1.1611	1.2568	1.4062	1.4618	*
1.6	1.2237	1.0959	1.2052	1.3193	1.4433	*
1.7	1.1800	1.0359	1.1566	1.3529	1.4261	*
1.8	1.1396	0.9785	1.1107	1.3272	1.4100	*
1.9	1.1021	0.9254	1.0671	1.3038	1.3950	*
2.0	1.0674	0.8756	1.0227	1.2817	1.3609	*
2.1	1.0352	0.8287	0.9862	1.2606	1.3676	*
2.2	1.0053	0.7846	0.9484	1.2405	1.3553	*
2.3	0.9775	0.7429	0.9122	1.2214	1.3432	*
2.4	0.9517	0.7036	0.8775	1.2011	1.3320	*
2.5	0.9277	0.6664	0.8441	1.1856	1.3214	*

$$M_y = 10^{-2} \cdot \delta q_0 R^2$$

Table 11. Numerical factor ξ_3 for moment M_z at middle of AC

$\frac{x}{R}$	0.2	0.4	0.6	0.8	1.0	
1.0	-4.80	-4.80	-4.80	-4.80	-4.80	Exact (6)
1.0	-4.8242	-4.8242	-4.8242	-4.8242	-4.8242	E.L.P.D.
1.1	-5.1871	-5.1945	-5.1403	-5.0856	-5.0275	*
1.2	-5.5146	-5.5302	-5.4422	-5.3295	-5.2322	*
1.3	-5.8039	-5.8914	-5.7304	-5.5580	-5.4109	*
1.4	-6.0530	-6.2160	-6.0666	-5.8713	-5.5751	*
1.5	-6.3605	-6.5300	-6.2717	-5.9761	-5.7283	*
1.6	-6.4260	-6.8273	-6.5267	-6.1694	-5.8700	*
1.7	-6.5492	-7.1097	-6.7724	-6.3512	-6.0022	*
1.8	-6.6306	-7.3771	-7.0092	-6.5253	-6.1259	*
1.9	-6.6711	-7.6294	-7.2378	-6.6917	-6.2417	*
2.0	-6.6710	-7.8665	-7.4386	-6.9510	-6.5507	*
2.1	-6.6347	-8.0894	-7.6720	-7.0036	-6.4535	*
2.2	-6.5604	-8.2952	-8.0782	-7.1507	-6.3305	*
2.3	-6.4523	-8.4867	-8.0775	-7.2822	-6.5423	*
2.4	-6.3118	-8.6532	-8.2702	-7.4286	-6.7294	*
2.5	-6.1416	-8.8246	-8.4565	-7.5605	-6.8121	*

$$M_z = 10^{-2} \cdot \delta q_0 R^2$$

C. 30 YOUSSEF AGAG

NOTATION

w = transverse deflection.
a = length of the nodal lines.
 ℓ = length or width of the plate.
 Δx = distance between the nodal lines.
E = modulus of elasticity.
 $t(x)$ = variable thickness of the plate.
 ν = poisson's ratio.
 $B(x)$ = variable flexural rigidity of the plate.
 B_k = flexural rigidity at any nodal line labelled k.
 B_0 = flexural rigidity at a reference nodal line.
 λ = ratio of rectangularity of the plate.
 α = thickness ratio.
 α_k = flexural rigidity ratio at any nodal line labelled k.
 $f_{m,k}$ = nodal line parameters.
 Y_m = chosen basic function.
q = load intensity.
 $[S]_m$ = square band matrix.
 $\{f\}_m$ = nodal line parameters vector.
 $\{P\}_m$ = load vector.

REFERENCES

1. CHEUNG,Y.K.: The Finite Strip Method in the Analysis of Elastic Plates with Two Opposite Simply Supported Ends. Proc.Inst.Civ.Eng., 40. 1968, p. 1-7
2. CHEUNG,Y.K.: Finite Strip Method Analysis of Elastic Slabs. Proc.ASCE, 94, EM6, 1968, p. 1365-1378
3. VLAZOV,V. : General Theory of Shells and its Application in Engineering, NASA TT F-69, April 1964
4. AGAG,Y. : Nodal Line Finite Difference Method for the Analysis of Elastic Plates with Two Opposite Simply Supported Ends. The Bulletin of the Faculty of Engineering, EL-Mansoura University, Vol.9, No.1. June 1984, p. C.136-C.147
5. AGAG,Y. : The Nodal Line Finite Difference Method with Iteration Procedure in the Analysis of Elastic Plates in Bending. The Bulletin of the Faculty of Engineering, EL-Mansoura University, Vol. 9, No.2, December 1984, p. C.8-C.22
6. TIMOSHENKO,S.P. and WOJNOWSKY-KRIEGER,S.: Theory of Plates and Shells, 2nd. Ed., McGraw Hill, New York, 1959